11507

TEST ROOM AND MEASUREMENT SYSTEM FOR ACTIVE DISPLACEMENT AIR DISTRIBUTION

Hannu Koskela[1], Timo Hautalampi[1], Esa Sandberg[2] and Mika Lindgren[3]

[1] Finnish Institute of Occupational Health, Turku, Finland
[2] Satakunta Polytechnic, Technology, Pori, Finland
[3] Detalmet Ky, Turku, Finland

ABSTRACT

A test room and measurement system were developed for the full-scale measurements of the active displacement air distribution. The room represents a 3-meter wide module of a larger hall. The requirements for the room included minimisation of the errors caused by air leaks, thermal conductance and flow obstacles. The measurement of the flow pattern is carried out with ultrasonic and thermal anemometers. Automated traversing system was built to move the sensors in the vertical symmetry plane of the room. The temperature gradient and boundary conditions of the test room are monitored with temperature and pressure sensors. Tracer-gas experiment is carried out in each test condition. The room was tested for air and thermal leakage and a calculation model was developed for leakage estimation. Measurements were carried out in one test condition to check the performance of the system and to compare the results given by different sensors. The test room and the experimental procedure were found suitable for the designed purpose.

Two other papers named *Convective Flows and Vertical Temperature Gradient with the Active Displacement Air Distribution* and *Behaviour of Convective Plumes with Active Displacement Air Flow Patterns* concerning this study are also submitted to be presented at the conference.

KEYWORDS

Air flow pattern, Air velocity, Full-scale experiments, Measuring instrumentation, Measuring techniques

INTRODUCTION

This study is a part of a research project named '*Convective Flows and Vertical Temperature Gradient within Active Displacement Air Distribution*'. The project was started in 1996 in order to determine guidelines for air flow rate dimensioning of the system. The objective of the present study was to develop a full-scale test room and measurement system for the laboratory experiments of the project. Other parts of the project are presented by Sandberg (1998) and Hautalampi (1998).

The test room was designed to represent a 3-meter wide module of a larger hall. The requirements for the room included minimisation of the errors caused by air leaks, thermal conductance and flow obstacles. For visualisation and video recording of the flow patterns, large windows were necessary. The experimental program of the project includes measurements of flow pattern in more than 100 test conditions. Therefore, an automated measurement and traversing system was needed.

METHODS

Test room and measurement system

The structure of the test room is shown in Figure1. The walls of the room are made of 50 mm thick polystyrene elements. Two active displacement supply devices are located symmetrically in the room at the height of 3 m. The length of the devices is the same as the width of the room. The units distribute supply air through small nozzles creating a nearly 2-dimensional flow pattern in the room. Exhaust air is taken through a perforated plate located in the middle of the ceiling. The room height can be changed between 4 m and 6 m by moving the ceiling.

The flow pattern is measured in the central plane of a half room. It is also visualised by creating a narrow light sheet in the measurement plane and recording smoke tests with video camera. The large windows are covered with polystyrene elements during the measurements.

The measurement of the air flow pattern is carried out with two Kaijo-Denki ultrasonic anemometers, which have an accuracy of ±0.02 m/s (Koskela 1996). The velocity vector components are averaged over a measurement period of 2-3 minutes. Hot bulb anemometers are included to complete the measurement grid of omnidirectional velocities. Temperature distribution is measured with Craftemp-thermistors. The thermistors were selected to give an accuracy of ±0.1°C at room temperature.

The traversing system was designed to cause minimal disturbance to the flow pattern. The supporting structure of the system is located near the wall at the distance of 1 m from the measurement plane. The sensors are traversed in the vertical symmetry plane creating a measurement grid with 0.2 m spacing. The components of the traversing measurement system are shown in Figure 2.

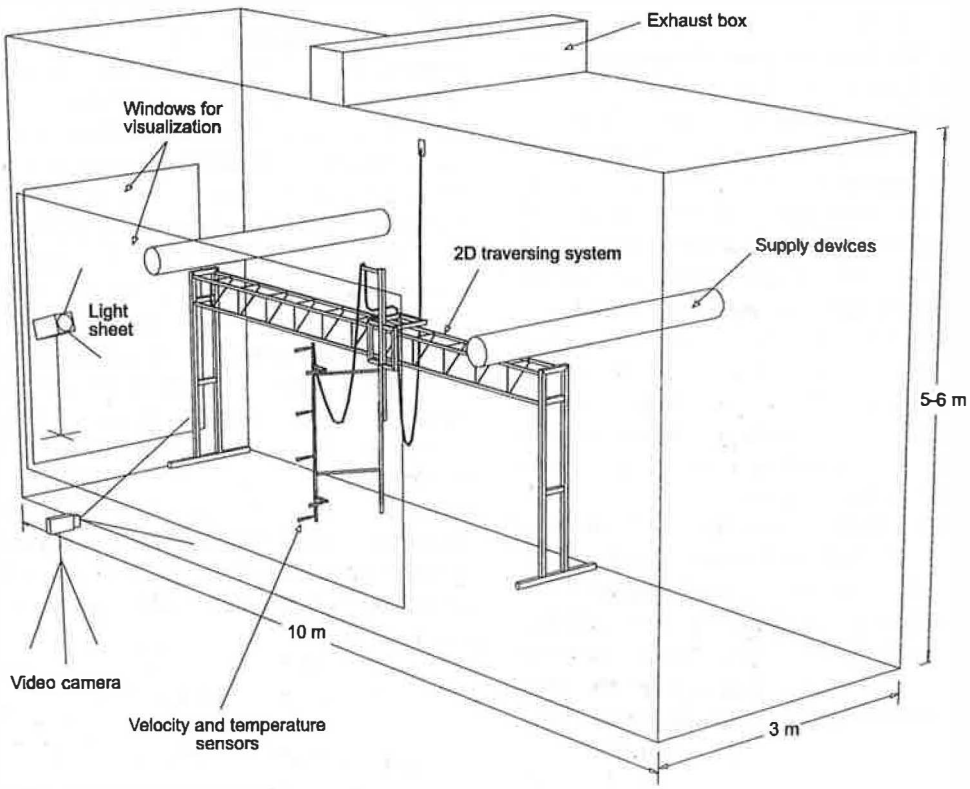

Figure 1 Structure of the test room and the traversing system.

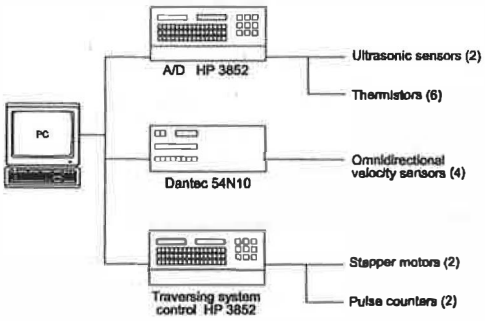

Figure 2 Components of the traversing measurement system.

The temperature gradient and the boundary conditions of the test room are monitored with thermistors. The temperature in the lower zone is measured with 5 radiation-shielded sensors, which are positioned at the height of 1.1 m at representative positions in the test room. When the test case is started, the positions of the sensors are checked to be outside of direct supply air flow or plume. The upper zone temperature is measured with 10 sensors located above the lower zone sensors at the distances of 0.3 m and 0.7 m from the ceiling. The temperature stratification is measured at one location with 0.5 m intervals. Other measurement points include supply air, exhaust air, stratification outside, surface temperatures of the test room and temperatures of the heat sources.

The supply flow rate is measured in the duct with an orifice plate and Furness PPC-500 pressure calibrator. The static pressure difference of the air terminal devices is measured with Micatrone MG 1000D pressure sensors and the pressure difference between the test room and the laboratory hall with Alnor MP6KSR pressure meter.

Tracer-gas experiment is carried out in each test condition with tracer injection to both supply air and heat sources. The air samples are taken from the breathing zone and upper zone through two perforated tubes in order to give average concentrations. The third sampling point is located in the exhaust. The concentrations are measured with Bruel&Kjaer 1302 infrared analyser. The data acquisition system is described in Figure 3.

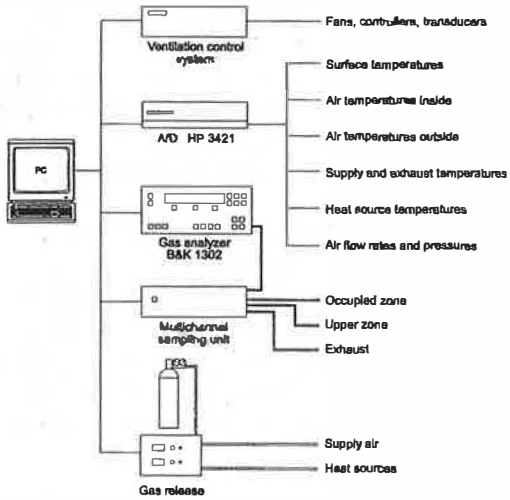

Figure 3 Data acquisition system for temperatures, pressures and tracer gas measurement.

Calculation of ventilation efficiency

The ventilation parameters are calculated from the measured mean temperatures, concentration levels and tracer gas decay curves with standard formulas (Ethridge 1996). The temperature effectiveness is calculated from

$$\varepsilon_T = \frac{T_s - T_e}{T_s - T_{lz}} \tag{1}$$

The corresponding parameter for contaminant concentration, local ventilation index in the lower zone is given by

$$\varepsilon_{lz} = \frac{C_e}{C_{lz}} \tag{2}$$

The supply air distribution is characterised by the local air-exchange index in the lower zone and the air-exchange efficiency

$$\varepsilon_{lz}^{a} = \frac{\tau_n}{\tau_{lz}} \tag{3}$$

$$\langle \varepsilon_a \rangle = \frac{\tau_n}{\langle \bar{\tau} \rangle} \tag{4}$$

Model for filtration leakage

A two zone model (Figure 4) is used for temperature stratification, because similar model is also used for modelling the air distribution in the project (Sandberg 1998). The height of the lower zone is assumed to be 4 m. In the air distribution measurements, the pressure difference between the test room and the surrounding hall is adjusted to zero near the floor by controlling the balance between supply and exhaust flow rates. Therefore the air leakage takes place through the ceiling and upper part of the walls. Also the temperature difference across the lower part of the wall is adjusted to close zero to minimise thermal leakage. If thermal stratification is higher in the test room than in the hall, which normally is the case, the leakage is always outwards from the test room.

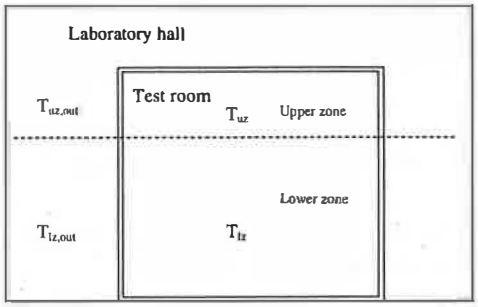

Figure 4 Two zone model for temperature stratification.

When the air temperature differences across the wall in the lower and upper zone are known, the pressure difference across the wall can be calculated from formula (Ethridge 1996)

$$\Delta P = \frac{\rho g}{T}\left(\Delta T_{lz} H_{lz} + \Delta T_{uz} H_{uz}\right) \qquad (5)$$

where ΔT_{lz} and ΔT_{uz} are the air temperature differences in the lower and upper zones and H is the corresponding zone height. The filtration air flow rate due to this pressure difference, and the corresponding heat flow rate, can then be calculated according to the pressurisation results from formulas

$$q_f = \alpha \Delta P^{\beta} \qquad (6)$$

$$Q_f = q_f c_p \rho \Delta T_f \qquad (7)$$

where q_f is the filtration air flow rate and ΔT_f is the temperature difference between infiltration and exfiltration air.

Model for conductive leakage

If the surface temperatures are known, the conductive leakage through the walls can be calculated from

$$Q = Q^{''} A = \lambda A \frac{(T_{w,in} - T_{w,out})}{L} \qquad (8)$$

The 50 mm thick polystyrene wall elements have a thermal conductivity λ of 0.03 W/mK. The ceiling is made of the same insulation elements, but has also a metal framework with total surface area of 3 m^2. The floor has a 20 mm chipboard plate above 30 mm insulation elements.

An estimate of the conductive leakage based on the air temperatures of lower and upper zones is also needed in the project. Because the total heat transfer coefficient U of the wall is mainly determined by the insulation element, a simplified method is used for convection and radiation heat transfer of the wall surfaces. The convection heat transfer coefficient h_c is given a value 2 W/m^{2}K and the radiation heat transfer is estimated with a heat transfer coefficient h_r of 4 W/m^{2}K. The heat flow rate through the walls can then be calculated from formula

$$Q = Q^{''} A = U_{wall} A (T_{in} - T_{out})$$

$$U_{wall} = \left(\frac{L}{\lambda} + \frac{1}{h_{in}} + \frac{1}{h_{out}}\right)^{-1} \qquad (9)$$

$$= (1.7 + 0.17 + 0.17)^{-1} \frac{W}{Km^2}$$

The U-value for the wall element becomes 0.49 W/m^{2}K and for the ceiling frame 2.9 W/m^{2}K. Total heat flow rate is a sum of heat flow rates through the room surfaces. The temperatures T_{in} and T_{out} are known only in the upper and lower zones and the floor temperature outside is assumed to be the same as the temperature in the lower zone.

RESULTS

Air leakage measurement

The tightness of the test room was measured by pressurising the room with a fan and measuring the flow rate at different pressure levels. The results are shown in Figure 5. Formulas for air and heat flow rates for 5 m room height are following

$$q_f = 26\Delta P^{0.76}[l/s] \quad (10)$$

$$Q_f = 2.7(4\Delta T_{lz} + \Delta T_{uz})^{0.76}[W] \quad (11)$$

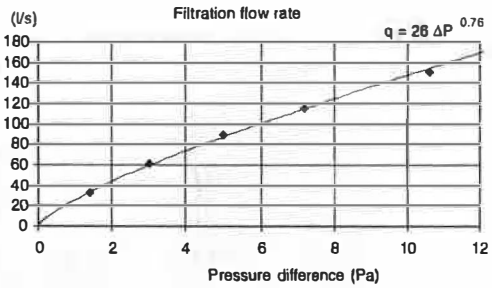

Figure 5 Results of the pressurisation measurement of the test room.

Test of the thermal leakage model

The calculation model was tested with two experiments. In the first experiment a convective heat source (85 % convection) of 620W was placed in the middle of the room on the floor. The temperatures were averaged for 1 hour after the heat source had been on for 10 hours. A similar experiment was carried out for a radiation heat source (70 % radiation) placed on an insulating element on the floor. The measured temperature differences ΔT_{air} and $\Delta T_{surface}$ and the calculated heat flow rates Q_c are shown in Table 1. The heat flow rates were calculated based on both surface temperatures and air temperatures. The heat balance in the experiments is summarised in Table 2.

The pressure difference across the wall was 1 Pa near the floor and zero at the ceiling level. This indicates that the lower part of the room is tighter than the movable ceiling. The pressure difference corresponds to the value calculated from formula (5).

The filtration air flow rate was measured with tracer gas experiment. The flow rate was small compared to the pressurisation test results because the pressure difference across the leaky ceiling was small. In the actual air distribution experiments, the filtration flow rate is higher because the pressure difference then occurs across the ceiling. This is due to the fact that the pressure difference across the lower part of the wall is adjusted to zero by the balance of the supply and exhaust flow rates.

Table 2 Heat balance for the 620 W sources.

	Convection source	Radiation source
Conduction heat flow rate	562 W	526 W
Filtration air flow rate	3 l/s	2 l/s
Filtration heat flow rate	20 W	14 W
Total heat flow rate	582 W	540 W
Error of heat balance	38 W	80 W

Table 1 Results of the thermal leakage measurement.

		Convection source				Radiation source			
	area (m^2)	ΔT_{air} (°C)	ΔT_s (°C)	$Q_{c,air}$ (W)	$Q_{c,s}$ (W)	ΔT_{air} (°C)	ΔT_s (°C)	$Q_{c,air}$ (W)	$Q_{c,s}$ (W)
Walls, upper zone	26	5.0	4.1	65	64	4.4	4.0	57	62
Walls, lower zone	104	5.1	4.2	264	262	4.6	3.7	238	230
Ceiling	27	5.0	4.1	67	66	4.6	4.0	62	65
Ceiling frame	3	5.0		44		4.6		41	
Floor	30		4.2	123	105		4.0	129	117
Total				562	541*			526	515*

*ceiling frame value included

In a typical measurement situation with supply air, the temperature stratification in the test room is 1.5 °C, the temperature difference across the wall zero in the lower zone and 1 °C in the upper zone. The estimated leakage values for such conditions are 5 l/s for exfiltration and 50 W for total thermal leakage.

Measurements in test conditions

The measurement system and the test procedure were studied in a test condition with moderate thermal flow rates. Convective heaters with total heating power of 1.0 kW were placed in the centre and at both ends of the room. The test conditions are given in Table 3. The temperature differences across the wall were small and therefore the pressure difference and thermal leakage were negligible. The ventilation cooling power calculated from supply and exhaust temperatures was 10 % higher than the total heating power. The measured and visualised air flow patterns are shown in Figures 6-8.

Table 4 Conditions of the test measurement.

Total heating power	1026 W
Supply air flow rate	168 l/s
Ventilation rate	4.02 1/h
Supply air temperature	21.2 °C
Exhaust air temperature	26.8 °C
Ventilation cooling power	1130 W
T_{in} lower zone	25.8 °C
T_{in} upper zone	26.7 °C
T_{out} lower zone	25.8 °C
T_{out} upper zone	26.8 °C

The standard deviations of the test conditions during the measurement period were 1.2 % for supply air flow rate and < 0.1 °C for all air and surface temperatures. The concentration curves of the tracer gas experiment are shown in Figure 9. Calculated values for ventilation efficiency parameters are shown in Table 4.

Figure 6 Visualised supply air flow pattern with 4.6 °C subtemperature of supply air.

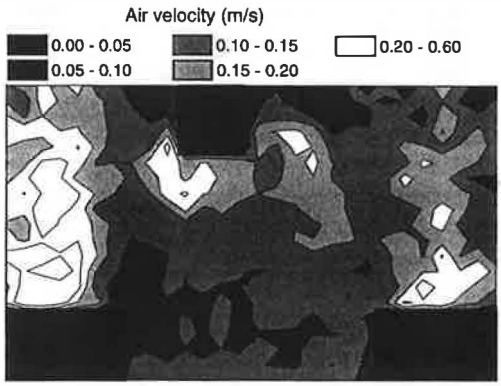

Figure 7 Omnidirectional velocity distribution measured with ultrasonic and hot bulb anemometers.

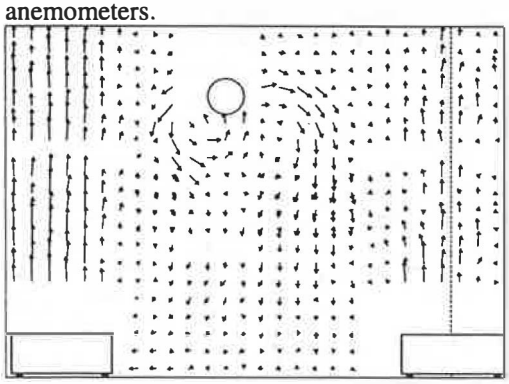

Figure 8 Velocity vector field measured with ultrasonic anemometers.

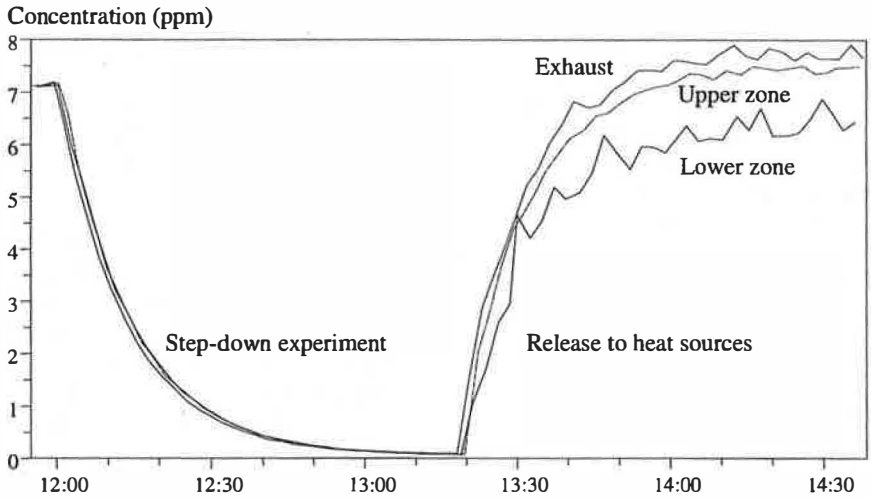

Figure 9 Concentration curves of the tracer gas experiment.

Table 4 Calculated values of ventilation efficiency parameters in the test case.

Temperature effectiveness	1.22
Ventilation index in the lower zone	1.20
Air-exchange index in the lower zone	1.07
Air-exchange efficiency	0.53

DISCUSSION

The test room was designed to represent a module of a larger hall with symmetrically placed supply devices. The symmetry planes of the hall are presented by side walls of the test room. The flow pattern in real buildings, however, is always complex and can not be adequately presented with symmetrical modules. Therefore, this kind of test arrangement is always a simplification of real conditions. The side walls of the test room affect the room flows, because air flows tend to be attached to walls. However, the effect of the side walls in these experiments is decreased by the fact that the main supply air flow pattern is always parallel to the side walls. The appearance of air flows in the perpendicular direction is checked with smoke tests. The presence of thermal plumes and their interaction with the supply air flow, however, makes the flow pattern in the test room more 3-dimensional.

In the project, a two zone model is developed for the thermal balance and contaminant flows of the room. Therefore, it is important to know the thermal behaviour and leakage of the test room components. In the test measurements the leakage model was able to estimate approximately 90 % of the thermal balance. The difference can be partly due to non-steady state conditions. After 10 hours the temperature levels had not fully reached the steady state.

The simplified model, which is based on mean air temperatures of the zones, gave similar heat flow rates in the test measurement as the calculation based on surface temperatures. For radiation heat sources with high heating power the situation is different. The wall temperature is increased by radiation and can become higher than the air temperature. In those cases the thermal leakage has to be calculated from the surface temperatures.

The thermal leakage in the test room was mainly (80-90 %) due to conduction through the surfaces. When the temperature difference across the wall is adjusted below 0.5 °C in the lower zone, the leakage values are normally within 5 % of the thermal flow

rate and air flow rate of the test case. The air leakage is normally outwards and mainly through the ceiling and can therefore actually be considered as a part of the exhaust flow rate.

The duration of the traversing measurement is typically 10 hours. In the test case, the supply air flow rate was maintained within 2 % and the supply temperature within 0.1 °C. The accuracy ±0.1 °C of the temperature sensors is sufficient for most test cases, but can become critical in cases with low heating power. The measurement accuracy of the mean temperatures in the supply and exhaust ducts is important for determination of temperature effectiveness.

In some test cases the flow pattern in the room was found to be unstable. When the supply air flow and thermal plumes interact, two different flow modes can sometimes occur. One flow mode can last for several hours and then change to another mode. In such cases, opposite velocity vectors are found in the results in some areas. This behaviour was also found with smoke tests. It can be caused by the symmetry of the test arrangement, which can lead to two symmetrical but opposite flow patterns. In that case the situation could be avoided by non-symmetrical placement of the heat sources.

ACKNOWLEDGEMENTS

The financial support of the Technology Development Centre Finland is greatly accepted.

REFERENCES

Ethridge, D. and Sandberg, M. (1996) *Building Ventilation: Theory and Measurement.* John Wiley & Sons, Chichester.

Sandberg, E., Koskela, H. and Hautalampi, T. (1998) Convective Flows and Vertical Temperature Gradient with the Active Displacement Air Distribution, submitted to *Proceedings of ROOMVENT '98.* Stockholm, Sweden

Hautalampi, T., Sandberg, E. and Koskela, H. (1998) Behaviour of Convective Plumes with Active Displacement Air Flow Patterns, submitted to *Proceedings of ROOMVENT '98.* Stockholm, Sweden

Koskela, H., Niemela, R., Hautalampi, T., Heikkinen, J. and Collineau, S. (1996). Use of ultrasonic anemometer for characterising room air flows. Indoor Air '96, proceedings of the 7th International Conference on Indoor Air Quality and Climate, Nagoya, Japan 1996, Volume 3, pp 845-850.